Journal of Soils and Sediments (2019) 19:2509–2519
https://doi.org/10.1007/s11368-019-02242-5

SOILS, SEC 5 • SOIL AND LANDSCAPE ECOLOGY • RESEARCH ARTICLE

Classification and characterization of bound water in marine mucky silty clay

Shuo Li[1] • Changming Wang[1] • Xianwei Zhang[2] • Linlin Zou[1] • Zhenxue Dai[1,3]

Received: 1 October 2018 / Accepted: 5 January 2019 / Published online: 15 January 2019

Abstract

Purpose Bound water has a large impact on physical and chemical properties of clay. The objective of this study was to investigate the contents, types, and physical properties of bound water and provide insights for understanding the thermal behavior and hydration process of the marine mucky silty clay under the control of bound water.

Materials and methods An integrated approach incorporating isothermal adsorption, thermogravimetric analysis (TGA), and specific gravity testing were developed to determine the contents and the boundaries of different types of bound water in Qingdao clay and investigate their physical characteristics.

Results and discussion Adsorption isotherm can be divided into two phases, which are the formation of strongly bound water and some capillary water under condition of $p/p_s < 0.9$ and the formation of weakly bound water in the coverage for $p/p_s > 0.9$. The initial dehydration temperatures of strongly bound water range between 87 and 92 °C in the hydrated clays under condition of $p/p_s < 0.98$. Weakly bound water starts to be released at temperatures near 60 °C and is completely removed at temperatures between 90 and 108 °C. Capillary water and free water are evaporated before 60 °C. The specific gravity of hydrated clay decreases linearly with adsorbed water contents. The volume of hydrated clay, volume of adsorbed water, and thickness of water film approximately linearly increase with adsorbed water contents.

Conclusions Quantitative determination and classification for bound water can be implemented through thermogravimetry (TG) and derivative thermogravimetry (DTG) curves. The physical properties of hydrated clay and bound water film are directly affected by the adsorbed water contents. The results may contribute to environmental and engineering risk assessment.

Keywords Bound water · Capillary water · Isothermal adsorption · Mucky silty clay · Thermogravimetric analysis

1 Introduction

Bound water in clay is composed of polar water molecules adsorbed on the surface of charged clay particles and differs in structure and properties from free water (Low 1979; Sposito and Prost 1982). Bound water is defined as the water in an electric double layer in general (Li et al. 2015). According to the distance and the attraction between water molecules and clay particle surfaces, bound water can be divided into strongly and weakly bound water. Bound water has a large impact on adsorption properties, thermogravimetric and mechanical behaviors (Ye et al. 2017) of clay due to its special physical and chemical properties. Clay has been commonly used as adsorption material (Bachmaf and Merkel 2010), subgrade, and barrier layer (Wong et al. 2017) in nuclear waste repository or landfill. Therefore, bound water involves chemistry, environment, and engineering problems such as sludge dewatering (Smith and Vesilind 1995; Yen and Lee 2001; Jin et al. 2004; Bian et al. 2018), soil remediation (Chen and Wu 1998), soil deformation (Chen et al. 2000), nuclear waste disposal (Sun et al. 2016), and gas reservoirs formation evaluation (Yuan et al. 2018). Investigations on the characteristics of

Responsible editor: Yi Jun Xu

✉ Changming Wang
wangcm@jlu.edu.cn

[1] College of Construction Engineering, Jilin University, Changchun 130026, China

[2] State Key Laboratory of Geomechanics and Geotechnical Engineering, Institute of Rock and Soil Mechanics, Chinese Academy of Sciences, Wuhan 430071, China

[3] Engineering Research Center of Geothermal Resources Development Technology and Equipment, Ministry of Education, Jilin University, Changchun, China

bound water have been of interest to the community of colloid chemistry (Sposito and Prost 1982), environmental science, soil science, geotechnical engineering, and oil-gas well engineering. Content determination, type classification, and physical properties of bound water can provide insights for understanding the hydration mechanism of clay, the migration law of bound water, and the influence of bound water on the physical and chemical properties of clay.

A few methods, individually or in combination, were applied to content determination and type classification of bound water on the surfaces of materials, such as centrifugal setting method (Yen and Lee 2001; Jin et al. 2004), X-ray diffraction, differential scanning calorimetry (DSC) (Liu et al. 2014), nuclear magnetic resonance (NMR) (Yuan et al. 2018), the permittivity method (Hilhorst et al. 2001), and the dilatometric method (Smith and Vesilind 1995; Wu et al. 1998; Bian et al. 2018). Multi-method solutions are recommended, for instance, the combination of the DSC method and conventional oven drying (Liu et al. 2014), the NMR in parallel with low-pressure nitrogen gas adsorption (Yuan et al. 2018). Generally, these methods embody the continuous enrichment and deepening of test techniques and provide a theoretical and technical basis for the quantitative study of bound water, but also have their disadvantages. The reliability of centrifugal setting method is questionable for the differences in sediment elasticities (Yen and Lee 2001). The dilatometrically measured bound water content is dependent on temperature, solids concentration, and other variables, which results in poor precision at low solids concentrations (Smith and Vesilind 1995). Nuclear magnetic resonance has deficiency in the demarcation for strongly and weakly bound water. X-ray diffraction and infrared spectroscopy place an emphasis on qualitative verification. Isothermal adsorption and thermogravimetric analysis (TGA) have their advantages in the description of clay-water interactions (Osipov 2012; Neuhaus 2013) and the determination of dehydration intervals, respectively. In recent years, TGA is widely applied to soils such as air-dry soils (Wang et al. 2011), loess (Li et al. 2015), cationic exchanged smectites (Kuligiewicz and Derkowski 2017), and soils for agricultural use (Kucerik et al. 2016, 2018) to determine their bound water contents. One major problem is the partition between strongly and weakly bound water. There are no uniform classification criteria for bound water based on TGA (Wang et al. 2011; Kucerik et al. 2016, 2018). The classification relying only on thermogravimetry (TG) curves is not enough to cope with the complex dehydration situations of some soils.

The physical and chemical properties of bound water can be further studied on the basis of determination for bound water content. Differences exist in structure, state, and properties among the water molecules at different binding sites (Martin 1962; Sposito and Prost 1982; Kasprzhitskii et al. 2016). Therefore, for easing computation and practical purposes, the quantitative descriptions are mostly at a holistic level of water film including the physicochemical properties of bound water film (mass, volume, density, thickness, strength, and so on) (Prost et al. 1998; Wu et al. 1998; Stepkowska et al. 2004) and their influence factors (soil texture, relative vapor pressure, adsorption time, and so on) (Stepkowska et al. 2004; Wang et al. 2011).

The thickness of the water film in clays is generally at the nanoscale, which contributes to the difficulties in quantitative classification and characterization of bound water through an individual technique (Smith and Vesilind 1995; Li et al. 2015). Therefore, the definitive and systematic approaches should be proposed at this stage based on multi-method collaboration. Furthermore, previous studies have paid much attention to the bound water in single clay minerals such as kaolinite (Chen et al. 2000; Kasprzhitskii et al. 2016), smectite (Kuligiewicz and Derkowski 2017), or illite; there is still a lack of detailed investigation for bound water in undisturbed mucky silty clay. One reason for that could be the complexity of clay (Barros et al. 2007). The surface of nature adsorbents, such as soils, is highly heterogeneous owing to their complexity of chemical composition and irregularities of physical structure (Chen and Wu 1998). The formation, distribution, and physical properties of bound water in undisturbed clay are different from those in single clay minerals.

This paper focuses on two main problems: one is the characterization of bound water in the special clay, Qingdao mucky silty clay and the other is the direct, effective, and accurate classification of bound water rather than vague definition. An integrated approach was developed incorporating isothermal adsorption, TGA, and specific gravity testing to solve above problems. Our aims were (1) to obtain the adsorption isotherm and built a phased adsorption model, (2) to measure the TGA laws of hydrated clays with different adsorbed water contents, (3) to determine the boundaries of strongly and weakly bound water based on the TG and derivative thermogravimetry (DTG) curves, and (4) to explore the physical properties of water film and the effect of bound water on clay properties. To the best of our knowledge, this work first presented the quantitative classification for bound water combining adsorption isotherm, TG, and DTG curves. In addition, this study provides theoretical values and reference functions for future use in research regarding environmental science and soil science topics.

2 Materials and methods

2.1 Soil samples

Soil samples called Qingdao clay in this paper were collected from a depth of between 6.0 and 13.0 m in the northern part of the Kiaochow Bay in Qingdao. The samples are undisturbed soils belonging to Quaternary marine sedimentary mucky silty

clay, ash black, pure, and delicate, in liquid plastic state. The physical properties of the samples are shown in Table 1. Grain-size distribution was measured by a combination of sieving and hydrostatic sedimentation methods, and the contents of sand, silt, and clay are 8.3%, 71.1%, and 20.6%, respectively. There is a general recognition that soil texture is the key factor determining soil water adsorption capacity (Wang et al. 2011). In general, mucky silty clay has higher clay content than sandy soils and silty soils and therefore higher specific surface area (S_{SA}). The ability of soil to adsorb water molecules is positively associated with its specific surface area (S_{SA}) (Chen and Wu 1998; Robinson et al. 2002; Dolinar 2014) and clay content (Li et al. 2015; Kucerik et al. 2018). Therefore, more attention should be paid to bound water of mucky silty clay in environmental and engineering projects.

The mineral composition of Qingdao clay was determined by an X-ray diffractometer (XRD) under the tube voltage of 40 kV and the measuring range of 2.6 to 45°. An X-ray fluorescence spectrum analyzer (XRF) was used to analyze the chemical composition. Table 1 depicts the mineral and chemical composition of Qingdao clay. Primary minerals include quartz, feldspar, calcite, and pyrite, with a total content of 82.6%. The abundance of primary minerals indicates that the weathering degree of Qingdao clay is not high. The primary minerals are often the main component of silt. The secondary minerals are all hydrophilic clay minerals including illite/smectite mixed layer, illite, chlorite, and kaolinite, with a total of 17.4%. Clay minerals are the material basis of bound water in soil. The non-clay minerals in the soils have no significant influence on the formation of bound water, but play a role in the process of capillary condensation (Li and Bo 1982). The content of SiO_2 is the highest, followed by Al_2O_3, Na_2O, K_2O, and Fe_2O_3. The high content of SiO_2 is due to the high content of quartz. Al_2O_3 and K_2O are related to feldspar, illite, and illite/smectite mixed layer.

2.2 Isothermal adsorption experiment

Isothermal adsorption can be used to determine the mass of adsorbed water on the surface of dried clay particles under different relative vapor pressures (p/p_s) (p being the vapor pressure in the desiccator and p_s being the saturated vapor pressure) and analyze the hydration law of clay. According to the components of Qingdao clay and the dehydration laws of clays in the relevant studies (Wang et al. 2011; Sun et al. 2016; Kucerik et al. 2018), bound water in Qingdao clay can be removed at the temperature range of 200 to 250 °C. The dehydroxylation of clay minerals occurs at 400 to 500 °C (Wang et al. 2011) and the surface of clay particles was unaffected before 400 °C (Huang et al. 2011). Considering these factors, air-dried clay was crushed, passed through a 0.075-mm sieve, and then dried at 250 °C to constant mass. Under the above treatment, 12 samples were obtained for isothermal adsorption experiment. The water vapor adsorption apparatus include 12 desiccators with a diameter of 150 mm and a height of 235 mm. The perforated ceramic plate in the desiccator divides the inner space into upper and lower chambers for sample placement and the control of relative vapor pressures, respectively. Twelve dried clay samples in weighing bottles were placed separately in the 12 desiccators equilibrated at $p/p_s = 0.1–1$. Relative vapor pressures ranging from 0.1 to 0.98 were controlled by sulfuric acid solution in the humidification chambers of desiccators, and the saturated vapor pressure ($p/p_s = 1$) was kept by distilled water (Table 2). Desiccators were placed in a thermotank at 25 °C, and the temperature was kept constant with an accuracy of 0.1 °C. Mass of each sample was measured every 24 h until constant. To reduce error, multiple experiments ($n = 4$) were executed on the samples at each relative vapor pressure. For each p/p_s, the final measurement result was the average of the testing values. The average values of the clay samples at each p/p_s were evaluated by two-sided t tests ($a = 0.05$).

2.3 Thermogravimetric analysis

Mass loss and temperature ranges corresponding to physical or chemical phase changes can be obtained through TG and DTG curves. A Netzsch STA 449F3 type synchronous thermal analyzer was used to test the thermal mass loss of specimens after adsorption equilibrium under different relative vapor pressures. Specimens were placed in crucibles and heated from 25 to 900 °C. (room temperature is 25 °C) under a flowing nitrogen atmosphere at a heating rate of 10 °C min^{-1}. Replicated experiments ($n = 4$) were performed on the specimens.

2.4 Specific gravity tests

Specific gravity tests were performed on 12 samples after adsorption equilibrium at each relative vapor pressure. The specific gravity of hydrated clay was determined by the pycnometer method (GB/T50123-1999 1999). A certain mass (m_0) of specimen was placed in a 50-mL pycnometer after adsorption equilibrium at certain p/p_s. The total mass of bottle and specimen was measured and half a bottle of anhydrous kerosene was injected into the pycnometer. The pycnometer was pumped for 3 h under one negative atmospheric pressure and then filled with anhydrous kerosene after vacuum pumping. The pycnometer containing sample was placed in a water bath at 25 °C in 30 min, and then removed and weighed (m_1). The pycnometer was washed and dried after the suspension had been discarded. The empty pycnometer was filled with anhydrous kerosene. The total mass of pycnometer and kerosene at 25 °C (m_2) was weighed according to the above method. Measurements for each sample were

Table 1 Physical parameters and composition of soil samples

Physical parameters		Mineral composition (%)		Chemical composition (%)	
Natural density ρ (g/cm^3)	1.95	Quartz	51.3	SiO_2	74.51
		Plagioclase	24.5	Al_2O_3	11.50
Specific gravity ρ_s (g/cm^3)	2.68	Potash feldspar	3.6	Fe_2O_3	2.40
		Calcite	1.9	FeO	0.71
Void ratio e	0.79	Pyrite	1.3	CaO	1.25
Liquid limit ω_L (%)	26.8	Illite/smectite mixed layer	13.1	MgO	1.13
				K_2O	2.43
Plasticity limit ω_P (%)	15.7	Illite	2.4	Na_2O	2.44
		Kaolinite	0.9	TiO_2	0.73
Specific surface area S_{SA} (m^2/g)	83.2	Chlorite	1.0	P_2O_5	0.07
				LOI	2.49

replicated four times with an accuracy of 0.0001 g. The specific gravity of hydrated clays can be calculated through m_0, m_1, m_2, and the density of kerosene.

3 Results and discussion

3.1 Adsorption isotherm

Adsorbed water content (q) refers to the mass of water released from sample by heating at 250 °C until there is no further mass loss, which is different from the water content determined by the conventional oven-drying method (i.e., heating the sample at 100–110 °C for 24 h). Figure 1 a presents the adsorption isotherm of Qingdao clay, adsorbed water contents increase with p/p_s. The morphology of adsorption isotherm manifested as irregular "S" type is not like Langmuir adsorption model (Langmuir 1918; Fan et al. 2013) but close to BET multilayer adsorption model (Fig. 1b).

The adsorption isotherm has two inflection points at $p/p_s = 0.3$ and $p/p_s = 0.9$, which define three intervals: $p/p_s < 0.3$, $0.3 < p/p_s < 0.9$, and $p/p_s > 0.9$. The values of q are 1.04% and 4.24% at two inflection points. When $p/p_s < 0.3$, adsorbed water contents gradually increase with p/p_s (Fig. 1c), the adsorption rule expressed by Eq. (1) accords with the Freundlich model (Freundlich 1906; Huang et al. 2013). The Freundlich isotherm is based on the assumption that adsorption occurs on a heterogeneous adsorption surface with different energies of adsorption (Tangaraj et al. 2017). The assumption matches the practical case of Qingdao clay at low relative vapor pressures.

$$q = 1.55(p/p_s)^{1/3.15} \quad (1)$$

In the coverage for $0.3 < p/p_s < 0.9$, adsorbed water contents steadily increase with p/p_s, and the adsorption model is in accordance with the expression:

$$q = 0.51 + 4.17(p/p_s)^2 \quad (2)$$

When $p/p_s > 0.9$, adsorbed water contents exponentially increase with p/p_s. The equation is as follows:

$$q = 4.08 + 9.41 \times 10^{-17} e^{39.59(p/p_s)} \quad (3)$$

Various adsorption stages correspond to different forms and binding sites of adsorbed water. Adsorbed water contents show convex increasing in the first stage ($p/p_s < 0.3$) because of monolayer coverage (Sing 1985). Water molecules are captured not only on the base surface but also at high-energy position of clay minerals such as crystal fracture and crystal angle. At this stage, water molecules are adsorbed on basal surface in groups with the formation of "island structure" rather than a uniform cover (Osipov 2012). Within the range of 0.3 to 0.9 p/p_s, water molecules slowly spread on the base surface of the clay minerals with the increase in p/p_s. Water molecules and clay minerals form entities by electrostatic attraction and hydrogen bonding in this process. In the coverage for $p/p_s < 0.9$, the major characteristic is the formation of strongly bound water, the adsorbed water mainly includes mono-hydrated layers (one plane of water molecules) and bi-hydrated layers (two planes of water molecules) on the basal surface of crystal layer (Cancela et al. 1997; Ferrage et al. 2005; Osipov 2012). Capillary condensation may also occur at contacts between particles at these low values of p/p_s (Prost et al. 1998). Above 0.9 p/p_s, the rapid growth in adsorbed water content corresponds mainly to multilayer adsorption associated with capillary condensation (Cases et al. 1997). The sharp increase also implies the emergence of a new form of bound water, namely, weakly bound water (Li and Bo 1982; Wang 2001; Wang et al. 2014).

Adsorption isotherm is widely used in environment, agriculture, and engineering areas because of its conciseness and practicability. Several characteristic water contents can be obtained from adsorption isotherm of Qingdao clay, such as the adsorbed water contents at $p/p_s = 0.6$ ($\omega_{0.6}$), $p/p_s = 0.9$ ($\omega_{0.9}$), and $p/p_s = 1$ (ω_1). The values of $\omega_{0.6}$, $\omega_{0.9}$ and ω_1 for Qingdao clay are 1.95%, 4.24%, and 18.78%, respectively. Water

Table 2 Relationship between p/p_s and concentration of sulfuric acid solution

p/p_s	0.1	0.2	0.3	0.4	0.5	0.6	0.7	0.8	0.9	0.95	0.98	1
Mass fraction (%)	64.45	57.76	52.45	47.71	43.10	38.35	33.09	26.79	17.91	11.02	6.00	0

molecules are adsorbed on basal surfaces of clay particles with the formation of an "island structure" rather than a uniform cover (Osipov 2012) when $q < \omega_{0.6}$. Formation of strongly bound water is main behavior in the coverage for $q < \omega_{0.9}$. When $q > \omega_{0.9}$, multilayer adsorbed water sharply increases in the three-phase system. The value of ω_1 is close to the plastic limit of clay, which is an important parameter of clay in engineering.

3.2 TG and DTG curves of hydrated clays

Different types of bound water correspond to different dehydration temperatures in the procedure of continuous heating because of the difference in connection forces. Figure 2 illustrates the TG curves of samples after adsorption equilibrium under different relative vapor pressures. Only five TG curves are listed because of space limitation. There are no obvious multistage steps in the TG curves, so a method based on derivative thermogravimetry (DTG, units of percentage mass loss $°C^{-1}$) is developed to divide strongly and weakly bound water. The DTG curve is superior to the TG curve because it improves the resolution of the TG curve. It can not only accurately reflect the initial and ultimate temperatures of the reaction but also confirm the maximum reaction rate. Based on the TG and DTG curves, the thermal reactions in stages on the hydrated clays can be effectively identified.

The DTG curves of hydrated clays all have obvious peaks in the temperature region between 25 and 250 °C. The peak of a DTG curve is the maximum of mass loss rate, and the temperature corresponding to the peak is defined as T_s. Mass loss rate decreases with temperature after mass loss rate has reached the peak, which indicates the dehydration stage of water in a new form, that is, strongly bound water. Therefore, T_s is the initial dehydration temperature of strongly bound water, and the content of strongly bound water can be obtained by the mass loss from T_s to 250 °C. The initial dehydration temperatures range between 87 and 92 °C for strongly bound water in the hydrated clays under condition of $p/p_s < 0.98$ but reach up to 108 °C at the saturated vapor pressure. The thermogravimetric interval is 108–250 °C for strongly bound water in the hydrated clay under the saturated vapor pressure.

Dehydration occurs at low temperatures from hydrated clay on account of capillary condensation. For dispersive non-clay minerals, water starts capillary condensation in the micropores even though p/p_s is relatively low. There is no weakly bound water in hydrated clays under condition of $p/p_s < 0.9$ because of the weak surface dissociation of non-clay minerals.

Another boundary temperatures T_w appear on the DTG curves in the temperature region of 58–62 °C for hydrated samples under condition of $p/p_s > 0.9$. The release of weakly bound water occurs at temperatures near 60 °C on the surface of solid particles such as mica and clay in general (Morin and Silva 1984). For high water content samples (Fig. 2d, e), particular dehydration processes occur in the temperature region between T_w and T_s (60–90 °C) with weakly bound water involved; capillary water and free water in samples have been lost before 60 °C.

Although numerous investigations of bound water in clay have been carried out based on TG curves, there are no uniform criteria to distinguish strongly and weakly bound water. Critical temperatures are one of the widely used methods (Eisenberg and Kauzmann 2005; Wang et al. 2011; Kucerik et al. 2016, 2018); however, various authors have specified different critical temperatures on weakly bound water that makes the bound water definition inconclusive. Another approach is to regard the inflection points on the TG curves as the demarcation points of strongly and weakly bound water (Wang 2001; Wang et al. 2014; Li et al. 2015). This method requires the TG curves which have apparent steps and inflection points in the dehydration intervals. For many clays and clay minerals, their TG curves manifest as smooth and continuous decline curves in their dehydration intervals, which causes difficulty in efficient partition. The classification method in this study is proposed under this background to provide a definitive and systematic approach to determine the types of bound water and their corresponding contents. The initial dehydration temperatures (T_w and T_s) are more intuitive and concrete than the ambiguous critical temperatures. Combination of TG and DTG curves has wider range of applications and higher resolution compared with the TG curves. In addition, TG and DTG curves reveal the details which are hidden in the adsorption isotherm, for example, the contents and the dehydration laws of capillary water under different relative vapor pressures. Multi-method combined testing is essential for determination and classification of bound water.

3.3 Types and boundaries of bound water

The results of TGA verify the change law of adsorption isotherm. We obtained the contents of strongly and weakly bound water, capillary water, and free water in hydrated clays under different p/p_s through the integrated approach (Table 3).

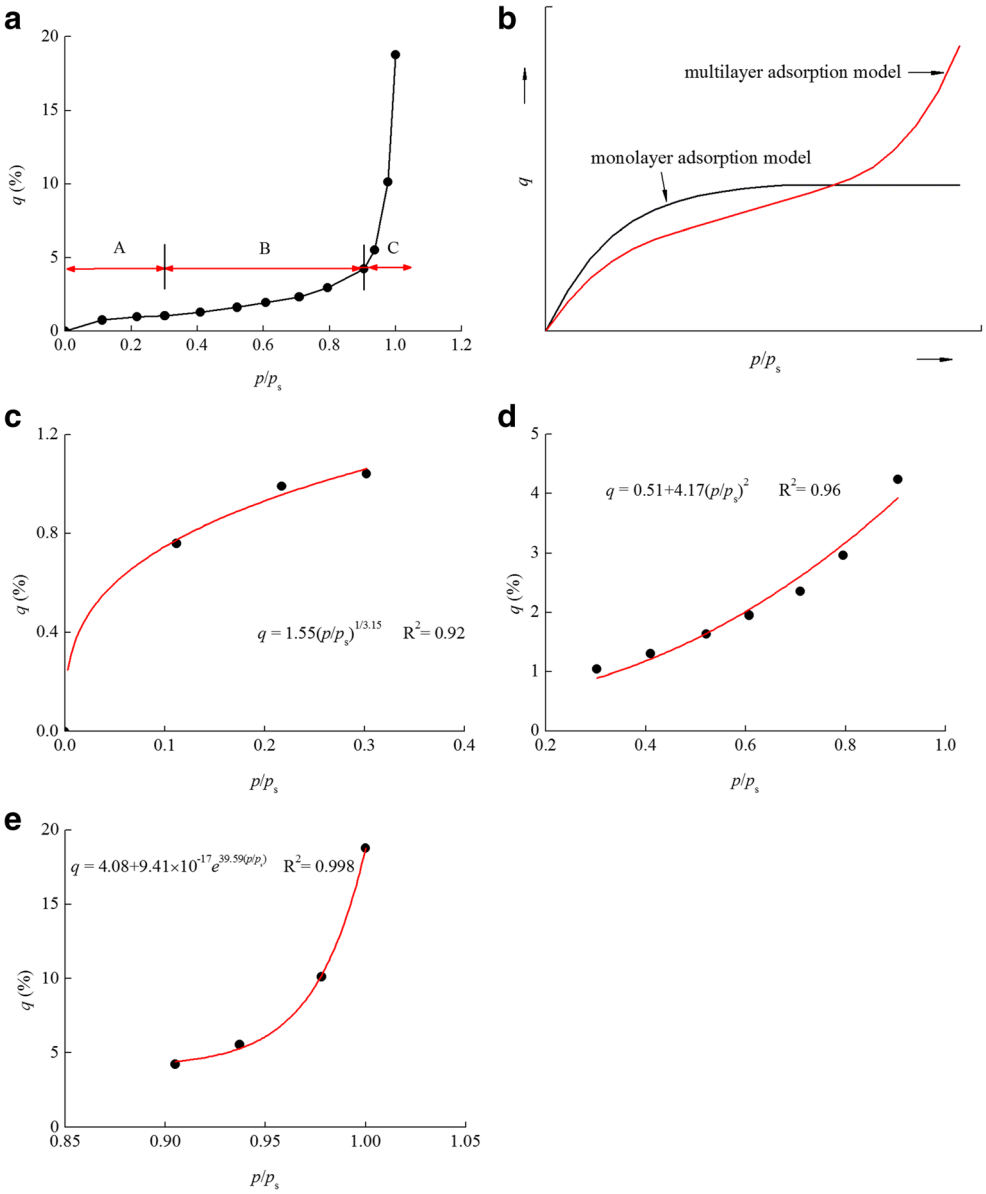

Fig. 1 Adsorption isotherms and adsorption models. (**a** Qingdao clay; **b** monolayer and multilayer adsorption; **c** $p/p_s = 0$~0.3; **d** $p/p_s = 0.3$~0.9; **e** $p/p_s = 0.9$~1.0)

Strongly bound water is closely associated with clay minerals with higher initial dehydration temperature (90–108 °C) and smaller dehydration rate than weakly bound water. The thermogravimetric interval of strongly bound water is 90–250 °C for the hydrated clays under condition of $p/p_s < 0.98$, 108–250 °C for the hydrated clays at $p/p_s = 1$.

Weakly bound water forms when $p/p_s > 0.9$. The DTG curves show that weakly bound water is completely removed at temperatures between 90 and 108 °C. The temperature range from 60 to 90 °C can be regarded as the thermogravimetric interval of weakly bound water in the coverage for $0.9 < p/p_s < 0.98$.

The existing p/p_s ranges are crossed for capillary water and bound water. Some capillary water already exists before the weakly bound water is fully formed. This phenomenon is also widespread in the vapor adsorption process of kaolin and illite (Li and Bo 1982). As transitional water between bound water and free water, capillary waters formed under different p/p_s correspond to different thermogravimetric intervals because of their difference in distribution location and connection force. Capillary water is equivalently attached to the strongly bound water layer when $p/p_s < 0.9$. When $p/p_s > 0.9$, capillary water is maintained by the force of meniscus in the three-phase system and is equivalently attached to the surface of weakly bound water layer. The thermogravimetric intervals of capillary waters vary by p/p_s because of the differences in positions, interactions, and water diffusion. The capillary water has properties similar to those of free water under condition of $p/p_s > 0.9$, such as low dehydration temperatures.

Figure 3 indicates the variation of different types of water with p/p_s. Capillary water contents increase with p/p_s and finally tend to a steady value of approximately

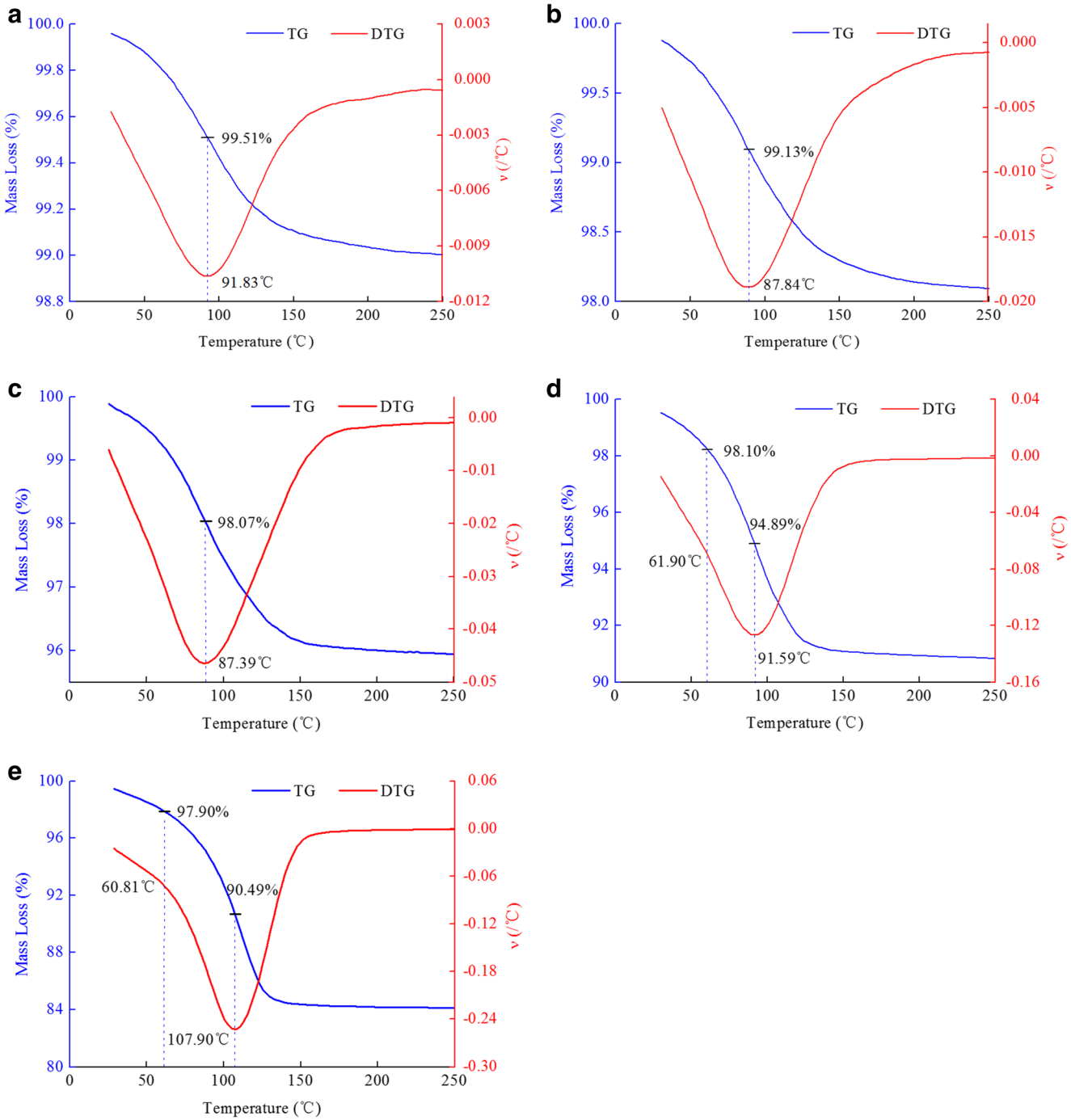

Fig. 2 Thermogravimetric curves for clay samples after adsorption equilibrium at different relative vapor pressures. (**a** $p/p_s = 0.3$; **b** $p/p_s = 0.6$; **c** $p/p_s = 0.9$; **d** $p/p_s = 0.98$; **e** $p/p_s = 1$)

2%. Weakly bound water occurs under condition of $p/p_s > 0.9$ with the maximum content of 8.84%. The formation of strongly bound water does not finish at $p/p_s = 0.9$ but continues with the increase in p/p_s. In the process of isothermal adsorption, the control factors of vapor adsorption are inward wedging forces of water molecules related to relative vapor pressures and the cohesion among clay particles. The cohesion impedes the inward wedging of water molecules. Some water molecules are stuck on the surface of particle aggregates, which result in some weakly bound water starting to form before the strongly bound water is completely formed. With the increase in p/p_s in the desiccators, inward wedging forces increase and water molecules move farther into the aggregates, which lead to more adequate hydration of clay minerals and the increase in contents of strongly bound water.

Table 3 Results of TGA and isothermal adsorption

Feature points	p/p_s	Isothermal adsorption q (%)	TGA					
			Dehydration (%)	ω_s[a] (%)	T_s (°C)	ω_w[b] (%)	T_w (°C)	ω_c[c] (%)
	0.11	0.76	0.73	0.42	89.78	–	–	0.31
	0.22	0.99	0.97	0.50	88.65	–	–	0.47
	0.33	1.04	1.01	0.52	91.83	–	–	0.49
	0.41	1.30	1.28	0.68	87.60	–	–	0.60
	0.52	1.63	1.60	0.83	87.42	–	–	0.77
$\omega_{0.6}$	0.61	1.95	1.95	1.06	87.84	–	–	0.89
	0.71	2.35	2.31	1.25	88.03	–	–	1.06
	0.80	2.96	2.95	1.46	87.50	–	–	1.49
$\omega_{0.9}$	0.91	4.24	4.22	2.21	87.39	–	–	2.01
	0.94	5.54	5.48	2.80	90.25	0.66	57.88	2.02
	0.98	10.12	10.08	4.46	91.59	3.58	61.90	2.04
ω_1	1	18.78	18.85	7.55	107.9	8.83	60.81	2.47

[a] Strongly bound water content, [b] weakly bound water content, [c] capillary and free water content

3.4 Physical properties of adsorbed water

The physical properties of hydrated clays and adsorbed water can be obtained by isothermal adsorption and specific gravity tests. The specific gravity of hydrated clays (ρ_{hc}) linearly decreases with adsorbed water contents (Fig. 4a). The volume of hydrated clay (V_{hc}) can be obtained by the specific gravity and the mass of hydrated clay. The formula is as follows:

$$V_{hc} = m_{hc}/\rho_{hc} \tag{4}$$

where m_{hc} is the mass of hydrated clay. It can be seen that V_{hc} is linearly correlated to adsorbed water contents (Fig. 4b).

The physical properties of adsorbed water were investigated including the volume (V_w) and density (ρ_w) of adsorbed water, and the assumed thickness of adsorbed water film (h_w). The parameters can be described by Eqs. (5–8) neglecting the volume change of dried clay particles with water contents. The method calculating V_w is expressed as Eq. (5).

$$V_w = V_{hc} - V_c \tag{5}$$

where V_c is the volume of dried clay. ρ_w can be described as given in Eq. (6).

$$\rho_w = m_w/V_w \tag{6}$$

where m_w is the mass of adsorbed water, and the value of m_w is equal to the difference between m_{hc} and the mass of dried clay (m_c) according to Eq. (7).

$$m_w = m_{hc} - m_c \tag{7}$$

Figure 4 c–e summarize the change rules of V_w and ρ_w. The volume of adsorbed water linearly increases with adsorbed water content. The density of the adsorbed water decreases with p/p_s. The values of ρ_w range from 1.30 to 1.32 g/cm^3 under condition of $p/p_s < 0.3$ and then fluctuate in the region between 1.25 and 1.27 g/cm^3 for $0.3 < p/p_s < 0.9$. When $p/p_s > 0.9$, ρ_w sharply decreases and finally drops to 1.16 g/cm^3 under the saturated vapor pressure. In general, ρ_w linearly decreases with adsorbed water content in the coverage for $p/p_s > 0.3$.

Water film thickness is an important parameter for studying the formation process and the scope of adsorbed water. In macroscale, the thickness of adsorbed water film is directly related to the mineral content (Osipov 2012), relative vapor pressure (Halsey 1948; Prost et al. 1998), temperature, and pressure (Morin and Silva 1984). In order to reflect the overall features of the non-uniform adsorbed water film in Qingdao clay, the assumed thickness of adsorbed water film (h_w) is used; h_w can be defined as the thickness of the water film when

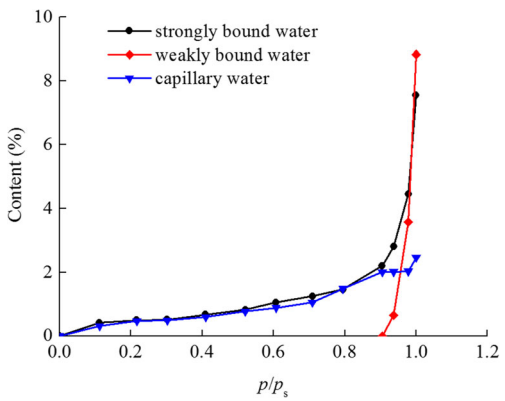

Fig. 3 Contents of various absorbed water under different relative vapor pressures

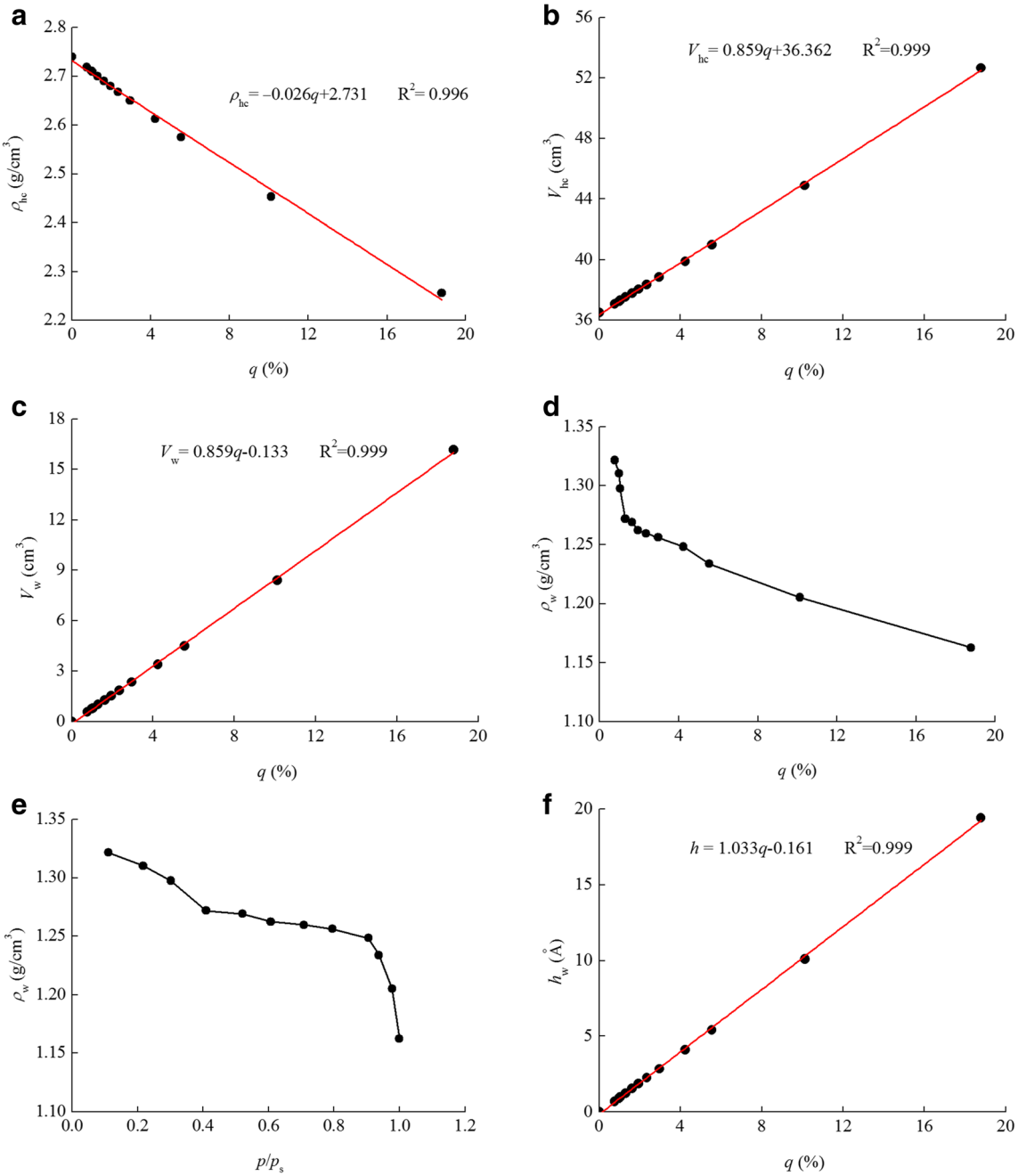

Fig. 4 Variation of physical parameters of hydrated clay and adsorbed water. (**a** ρ_{hc} versus q; **b** V_{hc} versus q; **c** variation in V_w with q; **d** variation of ρ_w with q; **e** variation of ρ_w with p/p_s; **f** relationship between h_w and q)

adsorbed water is evenly distributed on the surface of clay particles. The calculating formula for h_w can be expressed as:

$$h_w = V_w / S_{SA} \tag{8}$$

where V_w is the volume of adsorbed water, S_{SA} is the specific surface area of Qingdao clay, and the measured value of S_{SA} is 83.2 m^2/g.

Figure 4 f represents variation of h_w with adsorbed water contents; h_w linearly increases with q. When $p/p_s = 0.9$, h_w is 4.08 Å, which is 1.5 times of the diameter of the water molecule (2.77 Å). The variation of h_w can provide straightforward interpretation and verification for the process of vapor adsorption including "island structure" (Osipov 2012) and multilayer continuous adsorption. Sposito and Prost (1982) expounded that important structural difference in adsorbed water occurs in the first nanometer next to the smectite surface at low water content especially when the film of adsorbed water is not yet continuous. The data of h_w demonstrate the rule could

equally apply to Qingdao clay. Classical double-layer effects are obvious at high water content ($p/p_s > 0.9$). When q reaches the maximum value of 18.78%, h_w is 19.42 Å, which is nearly seven times of the diameter of a water molecule. The assay method for the physical properties of adsorbed water in the present study will be valuable in revealing and explaining the hydration mechanism of mucky silty clay and the impact of adsorbed water on the hydrated clay.

4 Conclusions

This study examined the vapor adsorption and thermogravimetric behaviors of Qingdao clay. Bound water is classified by the adsorption isotherm and DTG curves. The specific conclusions drawn from this study are as follows:

1. Adsorbed water contents increase with relative vapor pressure. The isothermal adsorption process can be divided into two phases with the demarcation point of 0.9 p/p_s. The main event is the formation of strongly bound water and capillary water under condition of $p/p_s < 0.9$. The weakly bound water forms when $p/p_s > 0.9$ with multimolecular adsorption.
2. The DTG curves of hydrated clays have obvious peaks in the temperature region between 25 and 250 °C. The initial dehydration temperatures of strongly bound water range between 87 and 92 °C in the hydrated clay under condition of $p/p_s < 0.98$, whereas they can reach up to 108 °C at the saturated vapor pressure. Weakly bound water starts to be released at temperatures near 60 °C and is completely removed at temperatures between 90 and 108 °C. The capillary and free water are evaporated before 60 °C.
3. Strongly and weakly bound water contents both increase with p/p_s. The existing p/p_s ranges are crossed for capillary water and bound water.
4. The specific gravity of the hydrated clay decreases with the adsorbed water content in a linear relationship. The volume of hydrated clay, volume of adsorbed water, and assumed thickness of water film linearly increase with adsorbed water contents. The density of adsorbed water decreases with p/p_s, ranging from 1.16 to 1.32 g/cm^3, and linearly decreases with absorbed water content under condition of $p/p_s > 0.3$. The maximum thickness of water film is seven times of the diameter of a water molecule.

Acknowledgments This work was supported by the Natural Science Foundations of China (Grant No. 41572257). The authors would like to thank Dr. Han Jing (College of Construction Engineering, Jilin University) for her contribution in data collection.

Compliance with ethical standards

Conflict of interest The authors declare that they have no conflict of interest.

Publisher's note Springer Nature remains neutral with regard to jurisdictional claims in published maps and institutional affiliations.

References

Bachmaf S, Merkel BJ (2010) Sorption of uranium (VI) at the clay mineral-water interface. Environ Earth Sci 63(5):925–934

Barros N, Salgado J, Feijóo S (2007) Calorimetry and soil. Thermochim Acta 458(1–2):11–17

Bian B, Zhang LM, Zhang Q, Zhang SP, Yang Z, Yang WB (2018) Coupled heating/acidification pretreatment of chemical sludge for dewatering by using waste sulfuric acid at low temperature. Chemosphere 205:260–266

Cancela GD, Huertas FJ, Taboada ER, Sanchez-Rasero F, Laguna AH (1997) Adsorption of water vapor by homoionic montmorillonites. Heats of adsorption and desorption. J Colloid Interface Sci 185(2): 343–354

Cases JM, Berend I, Francois M, Uriot JP, Michot LJ, Thomas F (1997) Mechanism of adsorption and desorption of water vapor by homoionic montmorillonite: 3. The Mg^{2+}, Ca^{2+}, Sr^{2+} and Ba^{2+} exchanged forms. Clay Clay Miner 45(1):8–22

Chen C, Wu S (1998) The influence of relative humidity on the adsorption of toluene by soils. Interpretation with the adsorption energy distribution functions. Chemosphere 37:1437–1444

Chen J, Anandarajah A, Inyang H (2000) Pore fluid properties and compressibility of kaolinite. J Geotech Geoenviron 126(9):798–807

Dolinar B (2014) Prediction of the soil-water characteristic curve based on the specific surface area of fine-grained soils. Bull Eng Geol Environ 74(3):697–703

Eisenberg D, Kauzmann W (2005) The structure and properties of water. Clarendon Press, Oxford

Fan JX, Wang YJ, Cui XD, Zhou DM (2013) Sorption isotherms and kinetics of Sb(V) on several Chinese soils with different physicochemical properties. J Soils Sediments 13(2):344–353

Ferrage E, Lanson B, Sakharov BA, Drits VA (2005) Investigation of smectite hydration properties by modeling experimental X-ray diffraction pattern. Part I Montmorillonite hydration properties. Am Mineral 90(8–9):1358–1374

Freundlich HMF (1906) Over the adsorption in solution. J Phys Chem 57: 384–470

GB/T50123-1999 (1999) Standard for soil test method. China Planning Press, Beijing (in Chinese)

Halsey GD (1948) Physical adsorption on nonuniform surfaces. J Chem Phys 16(10):931–937

Hilhorst MA, Dirksen C, Kampers FWH, Feddes RA (2001) Dielectric relaxation of bound water versus soil matric pressure. Soil Sci Soc Am J 65(2):311–314

Huang YT, Hseu ZY, Hsi HC (2011) Influences of thermal decontamination on mercury removal, soil properties, and repartitioning of coexisting heavy metals. Chemosphere 84:1244–1249

Huang Y, Liu Z, He Y, Zeng F, Wang R (2013) Quantifying effects of primary parameters on adsorption-desorption of atrazine in soils. J Soils Sediments 13(1):82–93

Jin B, Wilen BM, Lant P (2004) Impacts of morphological, physical and chemical properties of sludge flocs on dewaterability of activated sludge. Chem Eng J 98(1–2):115–126

Kasprzhitskii A, Lazorenko G, Sulavko S, Yavna V, Kochur A (2016) A study of the structural and spectral characteristics of free and bound water in kaolinite. Opt Spectrosc 121(3):357–363

Kucerik J, Demyan MS, Siewert C (2016) Practical applications of thermogravimetry in soil science. Part 4: relationship between clay, organic carbon and organic matter contents. J Therm Anal Calorim 123(3):2441–2450

Kucerik J, Tokarski D, Demyan MS, Merbach I, Siewert C (2018) Linking soil organic matter thermal stability with contents of clay, bound water, organic carbon and nitrogen. Geoderma 316:38–46

Kuligiewicz A, Derkowski A (2017) Tightly bound water in smectites. Am Mineral 102(5):1073–1090

Langmuir I (1918) The adsorption of gases on plane surfaces of glass, mica and platinum. J Am Chem Soc 40(12):1361–1403

Li SL, Bo ZZ (1982) Translation collection of adsorbed water in soil. Geological Publishing House, Beijing

Li YL, Wang TH, Su LJ (2015) Determination of bound water content of loess soils by isothermal adsorption and thermogravimetric analysis. Soil Sci 180(3):90–96

Liu H, Liu P, Hu H, Zhang Q, Wu Z, Yang J, Yao H (2014) Combined effects of Fenton peroxidation and CaO conditioning on sewage sludge thermal drying. Chemosphere 117:559–566

Low PF (1979) Nature and properties of water in montmorillonite-water system. Soil Sci Soc Am J 43(5):651–658

Martin RT (1962) Adsorbed water on clay: a review. Clay Clay Miner 9(1):28–70

Morin R, Silva AJ (1984) The effects of high pressure and high temperature on some physical properties of ocean sediments. J Geophys Res Solid Earth 89(B1):511–526

Neuhaus D (2013) Water adsorption and desorption pretreatment of surfaces increases the maximum amount of adsorbed water molecules by a multiple. Adsorption 19(6):1127–1135

Osipov VI (2012) Nanofilms of adsorbed water in clay: mechanism of formation and properties. Water Resour 39(7):709–721

Prost R, Koutit T, Benchara A (1998) State and location of water adsorbed on clay minerals: consequences of the hydration and swelling-shrinkage phenomena. Clay Clay Miner 46(2):117–131

Robinson DA, Cooper JD, Gardner CMK (2002) Modelling the relative permittivity of soils using soil hygroscopic water content. J Hydrol 255(1–4):39–49

Sing KSW (1985) Reporting physisorption data for gas/solid systems with special reference to the determination of surface area and porosity (recommendations 1984). Pure Appl Chem 57(4):603–619

Smith JK, Vesilind PA (1995) Dilatometric measurement of bound water in wastewater sludge. Water Res 29(12):2621–2626

Sposito G, Prost R (1982) Structure of water adsorbed on smectites. Chem Rev 82(6):553–573

Stepkowska ET, Pérez-Rodríguez JL, Maqueda C, Starnawska E (2004) Variability in water sorption and in particle thickness of standard smectites. Appl Clay Sci 24(3–4):185–199

Sun Q, Zhang WQ, Qian HT (2016) Effects of high temperature thermal treatment on the physical properties of clay. Environ Earth Sci 75(7): 610

Tangaraj V, Janot J-M, Jaber M, Bechelany M, Balme S (2017) Adsorption and photophysical properties of fluorescent dyes over montmorillonite and saponite modified by surfactant. Chemosphere 184:1355–1361

Wang PQ (2001) Study for quantitative analysis of water on clays and their hydration mechanism. Graduate School of Southwest Petroleum Institute (dissertation for PhD) (in Chinese)

Wang Y, Lu S, Ren T, Li BG (2011) Bound water content of air-dry soils measured by thermal analysis. Soil Sci Soc Am J 75(2):481–487

Wang TH, Li YL, Su LJ (2014) Types and boundaries of bound water on loess particle surface. Chin J Geotech Eng 36(5):942–948 (in Chinese)

Wong JTF, Chen Z, Chen X, Ng CWW, Wong MH (2017) Soil-water retention behavior of compacted biochar-amended clay: a novel landfill final cover material. J Soils Sediments 17(3):590–598

Wu CC, Lee DJ, Huang CP (1998) Bound water content and water binding strength on sludge flocs. Water Res 32(3):900–904

Ye C, Guo ZL, Cai CF, Wang JG, Deng J (2017) Effect of water content, bulk density, and aggregate size on mechanical characteristics of Aquults soil blocks and aggregates from subtropical China. J Soils Sediments 17(1):210–219

Yen PS, Lee DJ (2001) Errors in bound water measurements using centrifugal setting method. Water Res 35(16):4004–4009

Yuan YJ, Rezaee R, Verrall M, Hu S-Y, Zou J, Testmanti N (2018) Pore characterization and clay bound water assessment in shale with a combination of NMR and low-pressure nitrogen gas adsorption. Int J Coal Geol 194:11–21